ChemistryOpen

Full Papers
doi.org/10.1002/open.202100198

Chemistry Europe
European Chemical
Societies Publishing

Bidentate Lewis Acids Derived from *o*-Diethynylbenzene with Group 13 and 14 Functions

Jens Rudlof, Niklas Aders, Jan-Hendrik Lamm, Beate Neumann, Hans-Georg Stammler, and Norbert W. Mitzel*[a]

Starting from 1,2-diethynylbenzene, a series of bidentate Lewis acids was prepared by means of hydrometalations, in particular hydrosilylation, hydroboration, hydroalumination and terminal metalation based on group 13 and 14 elements. In the case of terminal alkyne metalation, the Lewis-acidic gallium function was introduced using triethylgallium under alkane elimination. A total of six different Lewis acids based on a semiflexible organic scaffold were prepared, bearing $-SiClMe_2$, $-SiCl_2Me$, $-SiCl_3$, $-B(C_6F_5)_2$, $-AlBis_2$ (Bis $=$ bis(trimethylsilyl)methyl) and $-GaEt_2$ as the corresponding functional units. In all cases, the Lewis acid functionalisation was carried out twice and the products were obtained in good to excellent yields. In the case of the twofold gallium Lewis acid, a different structural motif in the form of a polymer-like chain was observed in the solid state. All new bidentate Lewis acids were characterised by multinuclear NMR spectroscopy, CHN analysis and X-ray diffraction experiments.

1. Introduction

Compared to poly-Lewis bases (crown ethers, cryptands, spherands etc.),[1,2,3] poly-Lewis acids, that is, molecules bearing two or more Lewis-acidic functions, and their chemistry have only scarcely been investigated. Current research in the field of polydentate Lewis acids is being conducted on topics such as molecular recognition of guest molecules,[4] in catalytical processes[5] and also in optical applications.[6]

In 1960, pioneering work was presented by Holliday and Massey, having introduced ethyl-bridged diboranes for use in complexation experiments with Lewis-basic guest molecules.[7] These flexible bidentate Lewis acid systems often contained aluminium,[8] tin[9,10] or silicon[10] atoms as Lewis acid functions. The direct attachment of Lewis acid functions (e.g., based on mercury,[11] tin[12] and silicon[13]) to more rigid backbones such as benzene or naphthalene has also been investigated. For a more facile variation of the distance between the Lewis-acidic functions, spacer units have been used. As one example, relatively rigid ethynyl functions allow for a wide range of chemical modifications. Katz demonstrated a method for the construction of bidentate Lewis acids by terminal deprotonation of 1,8-diethynylanthracene and subsequent reaction with a chloroborane in a salt elimination reaction.[14] A terminal Lewis acid functionalisation of ethynyl groups under retention of the triple bond can also be achieved by metalation with alkylmetals under alkane elimination, first demonstrated by Jeffery and Mole, using trimethylgallium.[15]

We were able to use this elegant, often quantitatively proceeding method to introduce Lewis acid functions based on gallium, aluminium and indium atoms to different (partially-) organic frameworks.[16] Besides salt elimination and alkane elimination, hydrometalation is a further and frequently used procedure for introducing Lewis acid functions. The addition to the triple bond usually takes place regioselectively, frequently in excellent yields and under optimal atom economy. The resulting vinyl systems are more flexible than the alkynyl-based systems.

In this context, Uhl and co-workers reported hydroaluminations of suitable tri- and tetraalkynes.[17] Related reactions gave access to so-called molecular capsules by hydrogallation of alkynyl-substituted benzene derivatives and subsequent alkane elimination.[18] Recently, we reported the synthesis of a series of directed, bidentate and semiflexible Lewis acids based on an alkynyl-substituted anthracene backbone in which the Lewis acid functions are introduced by means of hydrosilylation and hydroboration.[19]
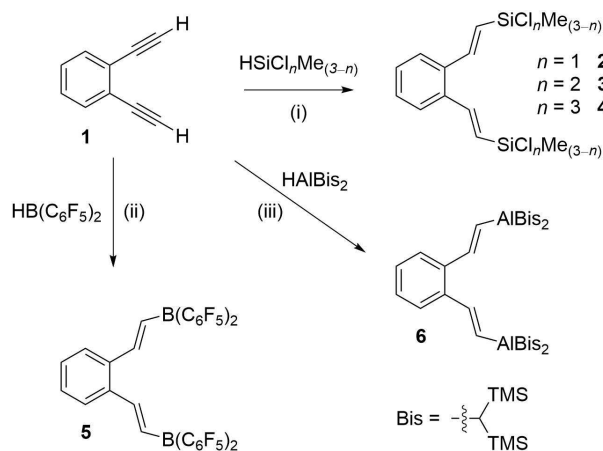
Synthetic access to tridentate acceptor systems by Lewis acid functionalisation has also been demonstrated. The hydrosilylation of 1,3,5-triethynylbenzene backbones afforded a poly-Lewis acid with large Si···Si distances [9.708(3), 8.662(3), 10.464(2) Å].[20]

In this work, we report the preparation of a series of directed, bidentate Lewis acids based on a 1,2-diethynylbenzene framework. Using efficient preparative routes for Lewis-acidic functionalisation, that is, hydrometalation and terminal metalation under alkane elimination, we disclose an easy-to-perform platform that can easily be functionalised with different Lewis-acidic groups.

ChemistryOpen

Full Papers
doi.org/10.1002/open.202100198

**Chemistry
Europe**
European Chemical
Societies Publishing

2. Results and Discussion

1,2-Diethynylbenzene (**1**), the organic backbone for all poly-Lewis acids discussed in this work, was synthesised according to protocols that had previously been reported.[21]

Scheme 1. Overview of synthesis routes starting from precursor **1** to products **2**–**6** via hydrometalation reactions. Reagents and conditions: (i) HSiCl$_n$Me$_{(3-n)}$ [$n=1$–3], Et$_2$O, Karstedt's cat., r.t., quant.; (ii) HB(C$_6$F$_5$)$_2$, benzene, r.t., 5 min, quant.; (iii) HAlBis$_2$, n-hexane, r.t., 15 min, quant.

2.1. Hydrosilylation with HSiClMe$_2$, HSiCl$_2$Me, HSiCl$_3$

The organic framework **1** was converted into terminally silylated species using HSiClMe$_2$, HSiCl$_2$Me and HSiCl$_3$ in presence of Karstedt's catalyst in hydrosilylation reactions (Scheme 1). Compounds **2**, **3** and **4** were obtained almost analytically pure and in virtually quantitative yields ($>99\%$) after removing all volatiles under reduced pressure. All products were characterised by multinuclear NMR spectroscopy and CHN analysis (for copies of all spectra, s. Supporting Information). The high *trans*-selectivity of the hydrosilylation reactions is confirmed by the large coupling constant ($^3J_{H,H} \approx 18$ Hz) of the vinylic proton resonances. The ^{13}C{^{1}H} NMR spectra show the anticipated number of resonances. The ^{29}Si{^{1}H} NMR spectral shifts of the silylated 1,2-derivates decrease from $\delta = 18.3$ ppm (**2**) to 17.1 ppm (**3**) and -2.9 ppm (**4**). A similar trend for these groups has been observed in previous studies.[19,20,22] Selected ^{1}H and ^{29}Si{^{1}H} NMR chemical shifts of the silyated species **2**–**4** measured in C$_6$D$_6$ at 298 K are listed in Table 1.

Crystals suitable for X-ray diffraction experiments for compounds **2**–**4** were obtained by sublimation. The molecular structures in the crystalline state of **2**–**4** are depicted in Figures 1 and 2. Figure 1 shows, as one example, the molecular structure of **2**. The structures of **3** and **4** are very similar (for comparison see also Figure 2 and Table 2). 1,2-Bis[(*E*)-2-(chloro-dimethylsilyl)vinyl]benzene (**2**) crystallises in the monoclinic space group $P2_1/c$ with four molecules in the unit cell. 1,2-Bis[(*E*)-2-(dichloromethylsilyl)vinyl]benzene (**3**) and 1,2-bis[(*E*)-2-

Table 1. Selected ^{1}H and ^{29}Si{^{1}H} NMR chemical shifts [ppm] of compounds **2**–**4** in C$_6$D$_6$ at 298 K.

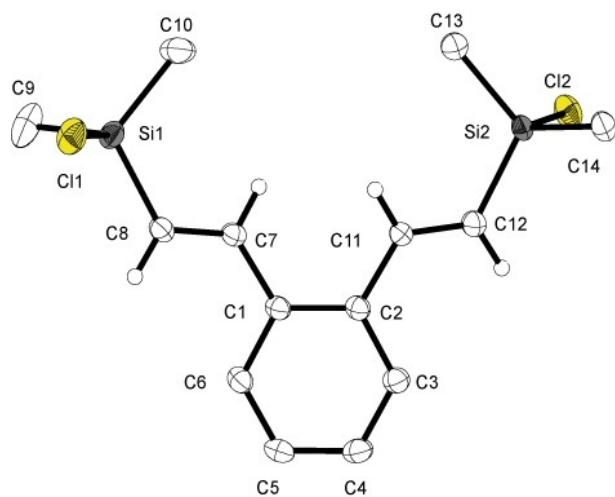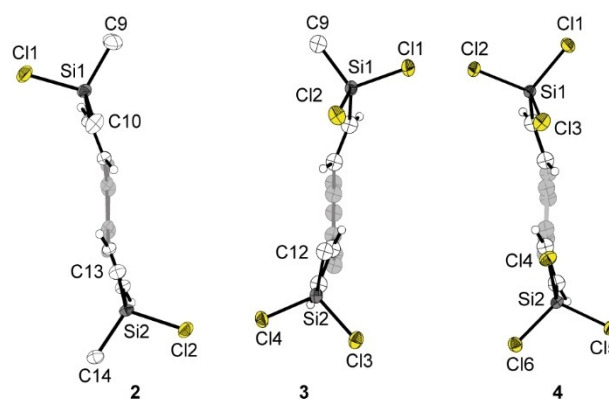| Compound	n	SiCl$_n$Me$_{[3-n]}$	C—CH=	=CHSi$_n$Me$_{[3-n]}$
2 (SiClMe$_2$)	1	18.3	7.43	6.22
3 (SiCl$_2$Me)	2	17.1	7.44	6.05
4 (SiCl$_3$)	3	−2.9	7.49	5.97

Figure 1. Molecular structure of **2** in the crystalline state. Displacement ellipsoids are drawn at the 50% probability level. Hydrogen atoms of the backbone and the methyl substituents are omitted for clarity. Selected bond lengths [Å] and angles [°]: C(1)—C(2) 1.415(4), C(1)—C(6) 1.404(4), C(1)—C(7) 1.479(3), C(7)—C(8) 1.336(4), C(8)—Si(1) 1.847(3), Si(1)—C(9) 1.852(4), Si(1)—Cl(1) 2.091(1), C(5)—C(6)—C(1) 121.4(3), C(6)—C(1)—C(2) 118.9(2), C(2)—C(1)—C(7) 121.4(2), C(8)—C(7)—C(1) 125.3(2), C(8)—Si(1)—C(9) 113.2(2), C(7)—C(8)—Si(1) 122.9(2), C(8)—Si(1)—Cl(1) 105.1(1), C(9)—Si(1)—Cl(1) 105.9(1), C(10)—Si(1)—C(9) 113.4(2), C(1)—C(7)—C(8)—Si(1) 176.1(2), C(1)—C(7)—C(8)—C(9) −176.1(2), C(6)—C(1)—C(7)—C(8) −24.0(4).

Figure 2. Molecular structures of **2**–**4** in the crystalline state, shown in a view along the benzene ring (benzene drawn in grey). Displacement ellipsoids are drawn at the 50% probability level. Minor occupied parts of disordered atoms, hydrogen atoms of the backbone and the methyl substituents are omitted for clarity. Selected function distances [Å] and bond angles [°]: (**2**) Si(1)···Si(2) 7.288(1), C(10)—Si(1)—C(9) 113.4(2), C(9)—Si(1)—Cl(1) 105.9(1), C(10)—Si(1)—Cl(1) 107.0(1); (**3**) Si(1)···Si(2) 7.120(1), C(9)—Si(1)—Cl(1) 109.3(6), C(9)—Si(1)—Cl(1) 106.6(6), Cl(2)—Si(1)—Cl(1) 107.4(1); (**4**) Si(1)···Si(2) 7.246(1), Cl(1)—Si(1)—Cl(2) 108.1(1), Cl(3)—Si(1)—Cl(1) 108.1(1), Cl(3)—Si(1)—Cl(2) 107.8(1).

ChemistryOpen

Full Papers
doi.org/10.1002/open.202100198

Chemistry Europe
European Chemical
Societies Publishing

Table 2. Selected bond angles and Si⋯Si distances of compounds **2**–**4**.

Compound	C(8)–C(7)–C(1)	C(6)–C(1)–C(7)–C(8)	Si(1)⋯Si(2)
2	125.3(2)°	−24.0(5)°	7.288(1) Å
3	126.0(2)°	27.1(8)°	7.120(1) Å
4	125.5(1)°	24.0(2)°	7.246(1) Å

(trichlorosilyl)vinyl]benzene (**4**) isostructurally crystallise in the monoclinic space group $P2_1/n$, each with four molecules in the unit cell. The solid-state structures of **2**–**4** confirm that the addition of the (chloro)methylsilanes to the C≡C triple bond proceeded almost identically in all cases, affording C=C double bonds with the vinylic H atoms adopting *trans* positions. This is indicated by the torsion angles of 180° [**2**: −176.1(2)°; **3**: 176.2(4)°; **4**: 176.5(1)°].

Furthermore, the C=C double bonds show a slight distortion and protrude out of plane of the benzene backbone, indicated by torsion angles of −24.0(5)° [**2**: C(6)–C(1)–C(7)–C(8)], 27.1(8)° [**3**: C(6)–C(1)–C(7)–C(8)] and 24.0(2)° [**4**: C(6)–C(1)–C(7)–C(8)]. The Si(1)⋯Si(2) distance between the Lewis-acidic Si atoms varies slightly from 7.288(1) Å (**2**) and 7.120(1) Å (**3**) to 7.246(1) Å (**4**); they are significantly smaller than in the silylated system based on 1,3,5-triethynylbenzene [9.708(3), 8.662(3),

10.464(2) Å].[20] The coordination geometry at the silicon atoms for compounds **2**–**4** is almost tetrahedral [angles ranging from 105.1(1)° to 113.4(2)° for **2**; 106.6(6)° to 114.3(5)° for **3**; 107.8(1)° to 111.9(1)° for **4**]. Deviations from the ideal tetrahedral angles are, as predicted by the VSEPR model, smaller for the Cl–Si–Cl angles and wider for the C–Si–Cl angles.[23]

A comparison of the structural parameters of compounds **2**–**4** with respect to the bond angles of the vinyl functions, the torsion angle which determines the deviation of the C=C double bond from the benzene plane and the distance between the silicon functions shows some similarities. The mentioned structural parameters are listed in Table 2.

2.2. Hydroboration with Piers' Borane

The organic framework **1** was converted into the bidentate boron Lewis acid 1,2-bis[(*E*)-2-(bis(perfluorophenyl)boranyl)vinyl]benzene (**5**) through hydroboration with $HB(C_6F_5)_2$, also known as Piers' borane (Scheme 1).[24] The reaction was carried out in benzene in which the desired product precipitated. Compound **5** was characterised using ^1H, ^{11}B, $^{13}C\{^1H\}$ and ^{19}F NMR spectroscopy and CHN analysis. The addition of Piers' borane to the triple bonds also led, with high selectivity, to the

Table 3. Crystallographic data for compounds **2**–**7** and **7a·Py**.

	2[a]	**3**[b]	**4**	**5**	**6**	**7**[c]	**7a·Py**
Empirical formula	$C_{14}H_{20}Cl_2Si_2$	$C_{12}H_{14}Cl_4Si_2$	$C_{10}H_8Cl_6Si_2$	$C_{40}H_{14}B_2F_{20}$	$C_{43}H_{89}AlN_2Si_8$	$C_{18}H_{24}Ga_2$	$C_{40}H_{34}Ga_2N_2$
M_r	315.38	356.21	397.04	896.13	898.83	379.81	682.13
λ [Å]	1.54184	1.54184	1.54184	1.54184	1.54184	1.54178	0.71073
T [K]	100.0(1)	100.0(1)	100.0(1)	100.0(1)	100.0(1)	200(2)	100.0(1)
$F(000)$	664	728	792	888	1968	388	700
Crystal system	monoclinic	monoclinic	monoclinic	triclinic	orthorhombic	triclinic	monoclinic
Space group	$P2_1/c$	$P2_1/n$	$P2_1/n$	$P\bar{1}$	$P2_12_12_1$	$P\bar{1}$	$P2_1/c$
a [Å]	7.0497(5)	6.9819(2)	6.89100(10)	7.5357(3)	9.33691(11)	9.2803(3)	12.0208(2)
b [Å]	19.098(1)	19.8788(5)	19.7231(2)	13.1948(4)	18.79123(18)	10.3414(4)	16.4703(3)
c [Å]	12.6982(7)	12.0692(3)	12.1059(2)	17.7171(5)	32.4263(3)	10.8038(4)	8.55220(10)
α [°]	90	90	90	83.552(3)	90	91.911(2)	90
β [°]	93.733(6)	102.732(2)	102.916(2)	82.068(3)	90	105.067(2)	101.970(2)
γ [°]	90	90	90	89.436(3)	90	115.800(2)	90
V [Å^3]	1706.01(18)	1633.92(8)	1603.71(4)	1733.72(10)	5689.25(10)	888.52(6)	1656.40(5)
Z	4	4	4	2	4	2	2
$\rho_{calcd.}$ [g cm^{-3}]	1.228	1.448	1.644	1.717	1.049	1.420	1.386
μ [mm^{-1}]	4.617	7.831	11.045	1.574	2.271	3.605	1.657
Θ_{max} [°]	152.712	153.33	152.986	152.612	153.2	132.8	64.184
Index ranges h	−8≤ h ≤8	−8≤ h ≤8	−8≤ h ≤8	−9≤ h ≤9	−11≤ h ≤10	−11≤ h ≤10	−17≤ h ≤17
Index ranges k	−23≤ k ≤23	−22≤ k ≤24	−24≤ k ≤24	−16≤ k ≤16	−14≤ k ≤23	−12≤ k ≤12	−24≤ k ≤23
Index ranges l	−15≤ l ≤15	−15≤ l ≤15	−15≤ l ≤13	−22≤ l ≤22	−40≤ l ≤36	−10≤ l ≤12	−12≤ l ≤12
Reflexes collected	10951	27801	45608	29785	26069	5324	49681
Independent reflexes	5996	3422	3370	7143	11706	2947	5581
R_{int}	0.0433	0.0627	0.0286	0.0323	0.0236	0.021	0.0376
Observed refl. [$I > 2\sigma(I)$]	5412	3169	3315	6021	11371	2629	4698
Parameters	168	181	195	615	511	208	200
R_1 [$I > 2\sigma(I)$]	0.0566	0.0326	0.0208	0.0425	0.0238	0.036	0.0315
wR_2 [$I > 2\sigma(I)$]	0.1833	0.0913	0.0547	0.1169	0.0588	0.099	0.0735
R_1 (all data)	0.0609	0.0350	0.0211	0.0509	0.0250	0.039	0.0423
wR_2 (all data)	0.2025	0.0944	0.0550	0.1239	0.0595	0.103	0.0779
GoF	1.154	1.112	1.039	1.016	1.021	1.040	1.049
ρ_{max}/ρ_{min} [e Å^{-3}]	0.57/−0.72	0.31/−0.45	0.30/−0.24	0.39/−0.28	0.32/−0.18	0.775/−0.284	0.70/−0.31
Flack parameter	–	–	–	–	0.006(8)	–	–
CCDC number	2098760	2098761	2098762	2098763	2098764	2098765	2098766

[a] Pseudo-merohedrically twinned crystal, ratio 58:42. Component 2 rotated by 180.0° around [0.99 −0.00 −0.11] (reciprocal) or [1.00 0.00 −0.00] (direct); [b] In each $SiCl_2Me$ group, the position of the carbon and of one chlorine atom are disordered in ratio of 51:49 or 89:11, resp.; [c] Disorder of Ga(2), C(15) to C(18) on two positions (84:16).

ChemistryOpen

Full Papers
doi.org/10.1002/open.202100198

Chemistry Europe
European Chemical
Societies Publishing

trans-product as is manifest by the large coupling constant of the vicinal vinylic protons ($^3J_{H,H} \approx 18$ Hz). The ^{11}B NMR spectrum displays a signal at 58.7 ppm. This compares well to shifts observed for similar compounds in previous studies.[16] In the ^{19}F NMR spectrum, three signals were observed, originating from the pentafluorophenyl substituents. The ^{13}C{^{1}H} NMR spectrum shows the expected number of signals, except for the *ipso*-carbon atoms of the pentafluorophenyl groups, which were not observed.

Compound **5**, precipitated from benzene solution, forms yellow crystals suitable for X-ray diffraction experiments. Figure 3 shows its molecular structure. It crystallises in the triclinic space group $P\bar{1}$ with two molecules in the unit cell. As with the previously discussed silylated species **2–4**, hydroboration of the triple bonds with Piers' borane also results in a *trans*-product, indicated by a torsion angle of $-170.4(2)°$ [C(1)–C(7)–C(8)–B(1)]. The C=C double bonds twist out of the benzene plane – similar
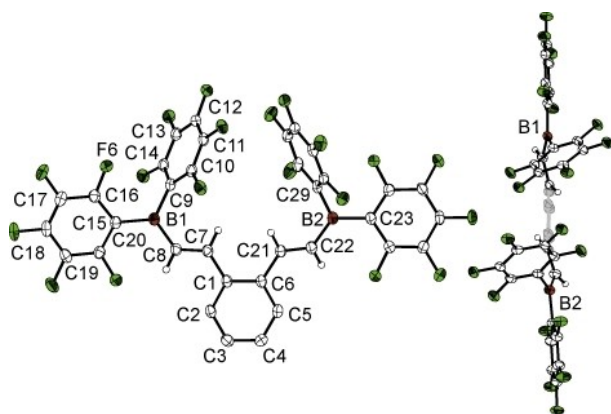

Figure 3. Molecular structure of **5** in the crystalline state. On the right, a view along the benzene ring (benzene drawn in grey) is shown. Displacement ellipsoids are drawn at the 50% probability level. A solvent benzene molecule and hydrogen atoms of the backbone, except those of the vinyl functions, are omitted for clarity. Selected bond lengths [Å] and angles [°]: C(1)–C(6) 1.420(2), C(1)–C(7) 1.470(2), C(7)–C(8) 1.349(3), B(1)–C(8) 1.538(3), B(1)–C(9) 1.586(3), B(1)–C(15) 1.584(3), C(16)–F(6) 1.337(2), C(6)–C(1)–C(7) 122.6(2), C(8)–C(7)–C(1) 124.1(2), C(7)–C(8)–B(1) 124.8(2), C(8)–B(1)–C(9) 119.5(2), C(8)–B(1)–C(15) 120.6(2), C(15)–B(1)–C(9) 119.9(2), F(6)–C(16)–C(15) 120.5(2), C(1)–C(7)–C(8)–B(1) $-170.4(2)$.
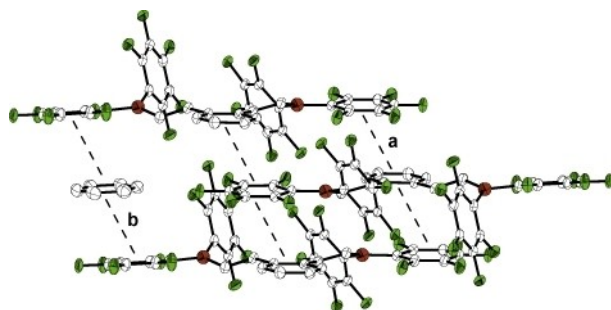

Figure 4. Stacking interactions between **5** and benzene. Displacement ellipsoids are drawn at the 50% probability level. Hydrogen atoms are omitted for clarity. Selected aryl-aryl interaction lengths and shortest C···C contact [Å]: (a) plane centroid [C(1)–C(6)] to plane centroid [C(15)–C(20)] distance 3.777(1) Å, C(15)···C(20) 3.386 Å; (b) plane centroid [C(23)–C(28)] to plane centroid [C(35)–C(40)] distance 3.738(1) Å, C(28)···C(35) 3.338(3) Å.

to compounds **2–4** – as indicated by the torsion angles of 21.5(3)° [C(2)–C(1)–C(7)–C(8)] and 25.7(3)° [C(5)–C(6)–C(21)–C(22)]. The distance between the Lewis-acidic boron functions is 7.329(3) Å [B(1)···B(2)]. Based on the angles of 119.5(2)° [C(8)–B(1)–C(9)], 120.6(2)° [C(8)–B(1)–C(15)] and 119.9(2)° [C(9)–B(1)–C(15)], the boron atoms have trigonal planar surroundings [$\Sigma < (C–B–C) = 360°$]. There is a different spatial orientation of the pentafluorophenyl substituents at the boron atom with respect to the benzene backbone. One of the pentafluorophenyl substituents is nearly co-planar with the benzene backbone, recognisable by a dihedral angle of 2.9(1)° [plane C(1–6) vs. C(15–20)]. The other substituent is clearly twisted by 64.1(1)° [plane C(1–6) vs. C(9–14)] relative to the benzene backbone.

Figure 4 shows aryl–aryl stacking interactions occurring between the benzene backbone of one molecule of **5** and the pentafluorophenyl substituent of another (distance a in Figure 4); the centroid-to-centroid distance is 3.777(1) Å. Further aryl–aryl stacking interactions are observed between the co-crystallised benzene solvent molecules and the pentafluorophenyl substituent (distance b in Figure 4) with a centroid-to-centroid distance of 3.738(1) Å.

2.3. Hydroalumination with HAlBis$_2$

In contrast to the previously described bidentate Lewis acids **2–5**, no electron-withdrawing substituents at the Lewis acidic atom are required to complex possible Lewis bases with the aluminium functions, since aluminium organyls have inherently a sufficiently high Lewis-acidity.

The reaction of the dialkyne precursor **1** with bis (bis[trimethylsilyl]methyl)aluminium hydride (HAl[CH(SiMe$_3$)$_2$] = HAlBis$_2$) provides the bidentate Lewis acid **6** in quantitative yield (Scheme 1). Compound **6** was characterised using multi-nuclear NMR spectroscopy and CHN analysis. The ^{1}H NMR data indicate a *trans*-arrangement of the vinylic protons ($^3J_{H,H} \approx 20$ Hz). Accordingly, the aluminium atom and the formerly aluminium-bound hydrogen atom are arranged *cis* to one another. This reflects the kinetically favoured hydroalumination product.[25,26] The ^{13}C{^{1}H} spectrum contains the anticipated number of resonances. The ^{29}Si{^{1}H} spectrum displays one signal at 17.1 ppm.

The non-complexed Lewis acid could not be obtained in crystalline form. Therefore, an adduct formation with pyridine (Py) was chosen to support the assumed structural connectivity. Suitable crystals of compound **6** were obtained by slowly concentrating a saturated solution of **6** in benzene, treated with two equivalents of pyridine.

1,2-Bis[(*E*)-2-(bis(bis(trimethylsilyl)methyl)aluminyl)vinyl] benzene (**6**) crystallises, as an adduct with one pyridine molecule, in the orthorhombic space group $P2_12_12_1$ with four molecules in the unit cell (Figure 5). Despite a slight excess of pyridine had been used during complex formation, we only observed formation of a 1:1 adduct between the bidentate Lewis acid **6** and one pyridine molecule. It is likely that the sterically demanding Bis-substituted (Bis = bis(trimethylsilyl)
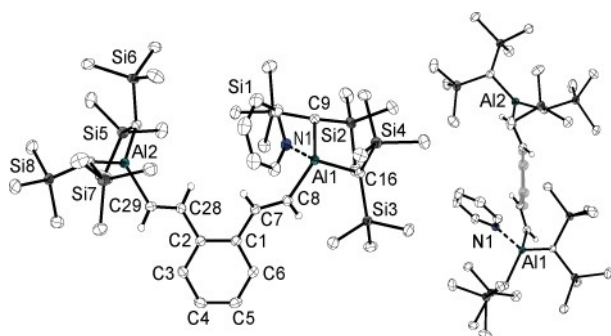
Figure 5. Molecular structure of **6**·Py in the crystalline state. On the right, a view along the benzene ring (benzene drawn in grey) is shown. Displacement ellipsoids are drawn at the 50% probability level. Hydrogen atoms, except those of the vinyl functions, are omitted for clarity. Selected bond lengths [Å] and angles [°]: C(1)–C(2) 1.411, C(1)–C(7) 1.483(3), C(7)–C(8) 1.342(3), Al(1)–C(8) 1.997(2), Al(1)–N(1) 2.028(2), Al(1)–C(9) 2.014(2), Si-(2)–C(9) 1.874(2), C(6)–C(1)–C(2) 118.5(2), C(2)–C(1)–C(7) 120.9(2), C(8)–C(7)–C(1) 127.8(2), C(7)–C(8)–Al(1) 128.9(1), C(8)–Al(1)–N(1) 100.3(1), C(8)–Al(1)–C(9) 112.5(1), Si(1)–C(9)–Al(1) 113.8(1), Si(1)–C(9)–Si(2) 112.8(1), C(1)–C(7)–C(8)–Al(1) −177.0(1), C(6)–C(1)–C(7)–C(8) 28.4(3).

Scheme 2. Synthesis of the bidentate gallium Lewis acid **7** by terminal metalation through alkane elimination. Reagents and conditions: (i) GaEt₃ (neat), r.t., 7 d, 88%.
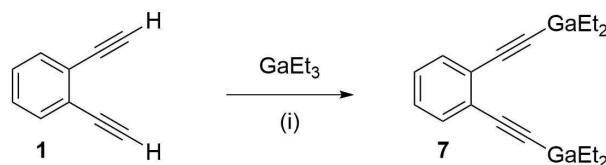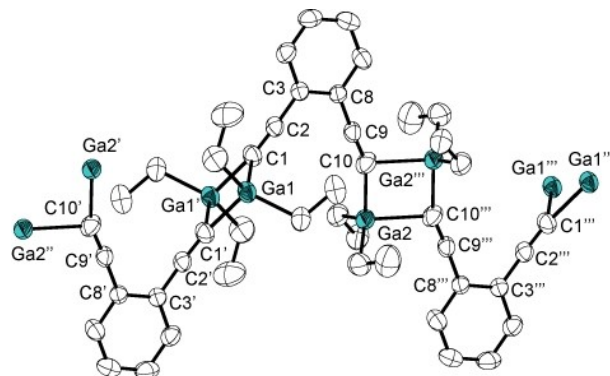
methyl) ligands prevent the second aluminium function to accept a pyridine molecule after saturation of the first one.

As already observed for the syntheses of the hydrosilylation and hydroboration products **2**–**5**, the hydroalumination of the triple bonds with HAlBis₂ occurs in *trans* position, indicated by the torsion angle of −177.0(1)° [C(1)–C(7)–C(8)–Al(1)]. The C≡C double bonds are significantly twisted out of the plane defined by the benzene backbone in comparison to compounds **2**–**5**; the torsion angles of 28.4(3)° [C(6)–C(1)–C(7)–C(8)] and 35.2(2)° [C(3)–C(2)–C(28)–C(29)] reflect the high spatial demand of the Bis groups. The distance between the Lewis-acidic functions in **6** is 7.514(1) Å [Al(1)···Al(2)] – the longest distance of all bidentate Lewis acids **2**–**5** described herein so far. The solid-state structure features one distorted trigonal planar coordinated aluminium atom, with bond angles at Al(2) ranging from 115.4(1)° to 125.7(1)° [Σ(C–Al–C) 359.9°]. The second aluminium atom Al(1), which participates in the adduct formation with pyridine, undergoes incomplete pyramidalisation resulting in bond angles ranging from 100.3(1)° [C(8)–Al(1)–N(1)] to 116.4(1)° [C(9)–Al(1)–C(16)].

Figure 6. Excerpt of the molecular structure of the polymer-like chains of **7** in the crystalline state. Displacement ellipsoids are drawn at the 50% probability level. Minor occupied disordered parts and hydrogen atoms are omitted for clarity. Selected bond lengths [Å] and angles [°]: Ga(1)–C(1) 2.142(3), C(1)–C(2) 1.209(4), C(2)–C(3) 1.425(4), C(3)–C(8) 1.414(3), C(8)–C(9) 1.428(4), C(9)–C(10) 1.216(4), C(10)–Ga(2) 2.069(3), C(2)–C(1)–Ga(1) 128.9(2), C(1)–C(2)–C(3) 176.7(3), C(8)–C(3)–C(2) 121.3(2), C(3)–C(8)–C(9) 121.1(2), C(10)–C(9)–C(8) 175.8(3), C(9)–C(10)–Ga(2) 157.5(2) (symmetry codes: '1−x, 2−y, 1−z; ''1+x, 1+y, 1+z; '''−x, 1−y, −z; ''''−1+x, −1+y, −1+z).

2.4. Terminal Metalation with GaEt₃

The reaction of the dialkyne compound **1** with triethylgallium by terminal metalation through alkane elimination provides the bidentate gallium Lewis acid 1,2-bis[(diethylgallanyl)ethynyl]benzene (**7**) under retention of the triple bonds (Scheme 2). The reaction was carried out in neat GaEt₃. Compound **7** was characterised by NMR spectroscopy and CHN analysis. The NMR spectra were recorded in THF-d₈ at ambient temperature. The ¹³C{¹H} NMR spectrum shows the anticipated seven resonances. Suitable crystals for structure elucidation by X-ray diffraction were obtained from benzene. Figures 6 and 7 show the molecular structure of **7**. It crystallises in the triclinic space group *P*1̄ with two molecules in the unit cell. The GaEt₂ unit is
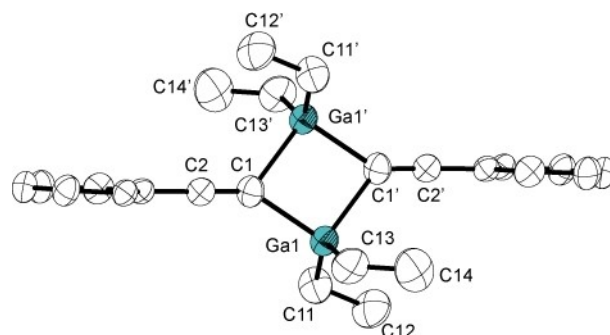

Figure 7. Excerpt of the molecular structure of **7** in the crystalline state. Displacement ellipsoids are drawn at the 50% probability level. Hydrogen atoms are omitted for clarity. Selected bond lengths [Å] and angles [°]: Ga(1)–C(1) 2.142(3), Ga(1)–C(1') 2.084(3), Ga(1)–C(11) 1.974(3), C(11)–C(12) 1.504(5), Ga(1)–C(13) 1.965(3), C(13)–C(14) 1.492(6), C(11)–Ga(1)–C(1) 105.0(1), Ga(1)–C(1)–Ga(1') 85.6(1), C(12)–C(11)–Ga(1) 113.2(3), C(13)–Ga(1)–C(1) 106.3(1), C(14)–C(13)–Ga(1) 116.1(3) (symmetry code: '1−x, 2−y, 1−z).

disordered over two positions with a ratio of 84:16; only the more strongly occupied part is discussed here. The molecules form a polymer-like chain in the solid state, with a displaced type of side-on coordination at the gallium–carbon axis which had previously been observed for related compounds.[27]

ChemistryOpen

Full Papers
doi.org/10.1002/open.202100198

Chemistry Europe
European Chemical
Societies Publishing

The following discussion concerns only the four-membered C(1)–Ga(1)–C(1')–Ga(1') ring. The gallium atoms are not located on the carbon–carbon axis of the triple bond and the C–C–Ga angles clearly deviate from 180° with values of 128.9(3)° [C(2)–C(1)–Ga(1)] and 145.4(3)° [C(2)–C(1)–Ga(1')]. The inner angles of the four-membered C(1)–Ga(1)–C(1')–Ga(1') ring are 85.6(1)° at C(1) and 94.4(1)° at Ga(1). The C≡C triple bond lengths are 1.209(3) Å [C(1)–C(2)] and 1.216(5) Å [C(9)–C(10)], which is within the normal range for a carbon triple bond.[28] The shortest Ga⋯Ga distance of a monomer unit is 2.870(1) Å
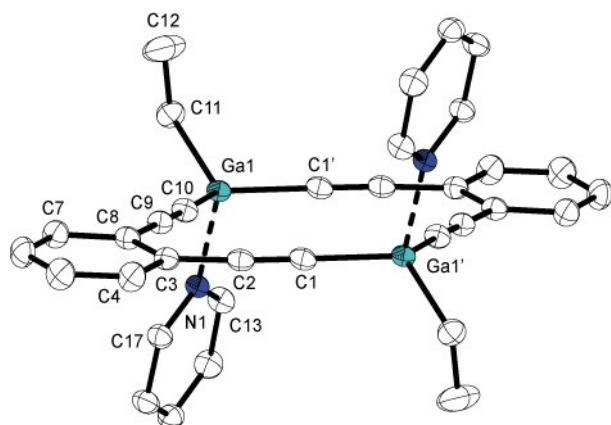

Figure 8. Molecular structure of **7a**·Py in the crystalline state. Displacement ellipsoids are drawn at 50% probability. Hydrogen atoms are omitted for clarity. Selected bond lengths [Å] and angles [°]: Ga(1)–N(1) 2.052(1), Ga(1)–C(1) 1.956(2), C(1)–C(2) 1.207(2), C(2)–C(3) 1.436(2), C(3)–C(8) 1.412(2), C(8)–C(9) 1.437(2), C(9)–C(10) 1.202(2), C(10)'–Ga(1) 1.949(2), C(1)–C(2)–C(3) 178.0(2), C(8)–C(3)–C(2) 120.6(1), C(3)–C(8)–C(9) 121.3(2), C(10)–C(9)–C(8) 177.0(2), C(9)–C(10)–Ga(1)' 176.4(2), C(10)'–Ga(1)–N(1) 100.4(1) (symmetry code: '1−*x*, 1−*y*, -*z*).
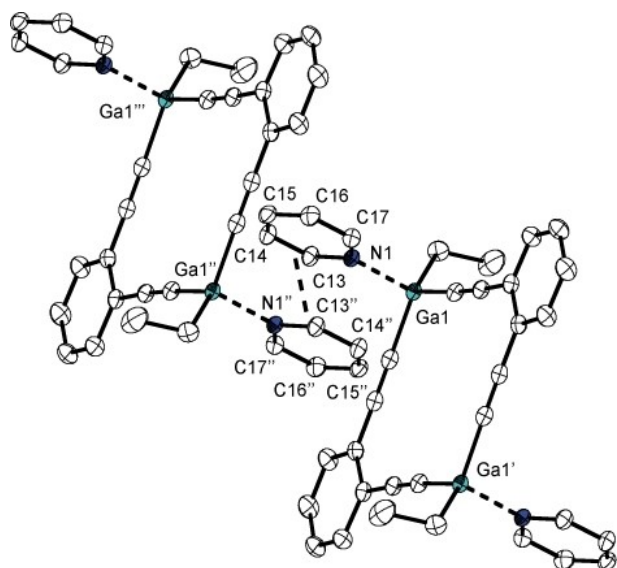

Figure 9. Aggregation of **7a**·Py in the crystalline state through aryl–aryl stacking. Displacement ellipsoids are drawn at the 50% probability level. Hydrogen atoms are omitted for clarity. Selected aryl–aryl interaction lengths and shortest C⋯C contact [Å]: plane centroid [C(15)–C(14)–C(13)–N-N(1)–C(17)–C(16)] to plane centroid [C(15")–C(14")–C(13")–N-N(1")–C(17")–C(16")] distance 3.787(1) Å, C(17)⋯C(16") 3.563(2) Å; (symmetry codes: '1−*x*, 1−*y*, −*z*; "1−*x*, 1−*y*, 1−*z*; "'*x*, *y*, 1+*z*).

[Ga(1)–Ga(1')]. The distances between the gallium atoms vary from 6.245(1) Å [Ga(1)–Ga(2)], 7.533(1) Å [Ga(1)–Ga(2''')], 5.563(1) Å [Ga(1')–Ga(2)] to 7.567(1) Å [Ga(1')–Ga(2''')].

The polymeric nature of **7** explains its insolubility in non-polar solvents such as benzene. However, these polymer-chains can be broken by the addition of donor atom-containing substances such as THF, which dissolves the compound.

In a dissolution experiment with the solvent mixture CD_2Cl_2/C_6D_6, pyridine was added into this suspension by slow diffusion. This did not afford the expected bis-pyridine adduct but led to a condensation of two molecules **7** under cleavage of $GaEt_3$ along with pyridine adduct formation. However, no useful quantities of the condensation product **7a** could be obtained in this way, and the compound could solely be characterised by X-ray diffraction experiments. Figures 8 and 9 show the molecular structure of **7a**·Py and its aggregation by aryl–aryl stacking. The ring structure crystallises at a centre of inversion in the monoclinic space group $P2_1/c$ with two molecules in the unit cell. The gallium functions are nearly in plane with the benzene backbone as shown by the torsion angle of 7.6(3)° [Ga(1)–C(8)–C(3)–Ga(1')]. The distance between the gallium function and the pyridine nitrogen atom is 2.052(1) Å [Ga(1)–N-(1)]. The gallium–gallium distance is 6.326(1) Å [Ga(1)–Ga(1')]. The coordination sphere at the gallium atoms is distorted tetrahedral, the underlying GaC_3 acceptor unit being incompletely pyramidalised by binding the pyridine donor. This can also be seen by the relatively small N–Ga–C angles like 102.1(1)° [C(1')–Ga(1)–N(1)] and relatively large angles C–Ga–C like 115.7(1)° [C(1')–Ga(1)–C(11)] and 112.5(1)° [C(1')–Ga(1)–C(10)]. Aryl–aryl stacking occurs between the pyridine units of **7a**·Py, apparent by a centroid-to-centroid distance of 3.787(1) Å shown in Figure 9.

As shown for compounds **6** und **7a**, the very accessible bidentate Lewis acids based on group 13 and 14 functions are suitable for host-guest experiments and can form adducts with Lewis basic substrates. Therefore, these model systems are capable of studying non-covalent interactions based on Lewis acid-to-base interactions in the context of supramolecular chemistry.

3. Conclusion

Starting from 1,2-diethynylbenzne **1**, a series of bidentate Lewis acids were synthesised by hydrometalation and terminal metalation. To introduce the Lewis-acidic functions based on group 13 and 14 elements, ethynyl precursor **1** was reacted in hydrosilylation, hydroboration, hydroalumination and terminal metalation reactions with triethylgallium. The bidentate Lewis acids were obtained in good to excellent yields and the structures in the solid state were elucidated by X-ray diffraction experiments. In the hydrometalation reactions (**2, 3, 4, 5, 6**), the addition to the triple bonds proceeded in *trans*-position in all cases and the Lewis-acidic functions occupy the position at the *β*-carbon atom of the resulting double bond. A different structural motif was obtained upon terminal metalation of precursor **1** with triethylgallium. The solid-state structure of **7**

ChemistryOpen

Full Papers
doi.org/10.1002/open.202100198

**Chemistry
Europe**
European Chemical
Societies Publishing

shows a polymer-like chain connected by digallacyclobutane units. In the presence of pyridine, a side reaction in the form of a condensation reaction led to the formation of a ring structure **7 a**·Py.

To study Lewis acid-to-base interactions in the context of supramolecular chemistry, easily accessible polydentate Lewis acid systems are needed. These should be free of heteroatoms and preferably have rigid, directed receptor functions, as these often show the highest selectivity towards Lewis-basic guests. This work demonstrates synthetic access to six novel bidentate receptors that are well suited as probe platforms for the study of weak, non-covalent interactions and can expand the field of supramolecular chemistry in the area of Lewis acid-to-base interactions.

Experimental Section

General. The synthesis of precursor **1** was described previously.[21] Chlorodimethylsilane, dichloromethylsilane and trichlorosilane were purchased from Sigma-Aldrich and used without further purification. Karstedt's catalyst was purchased from ABCR (3–3.5% Pt). HB(C_6F_5)$_2$[24] and HAlBis$_2$[29] were synthesised according to literature protocols. All reactions were carried out under an anhydrous atmosphere of nitrogen or argon using standard Schlenk or glovebox techniques and dried and degassed solvents (benzene from Na/K alloy, *n*-hexane and Et$_2$O from LiAlH$_4$). Pyridine was dried over sodium hydroxide plates at ambient temperature and then distilled. NMR spectra were recorded using a Bruker Avance III 500 HD spectrometer at room temperature (298 K). The chemical shifts (δ) are reported in ppm and are referenced to the solvent signals (C$_6$D$_6$: ^{1}H NMR $\delta = 7.16$ ppm, ^{13}C NMR $\delta = 128.06$ ppm; THF-d$_8$: ^{1}H NMR $\delta = 3.58$, ^{13}C NMR $\delta = 67.57$) or externally (^{11}B: BF$_3$·OEt$_2$; ^{19}F: CFCl$_3$; ^{29}Si: SiMe$_4$). CHN elemental analyses were performed with a HEKAtech EURO EA analyser (too low values for carbon are due to the known formation of silicon carbide or boron carbide).

General Procedure for Hydrosilylation Reactions: Precursor **1** was dissolved in a mixture of the corresponding (chloro)methylsilanes and diethyl ether. A drop of Karstedt's catalyst (3–3.5% Pt) was added and the resulting reaction mixture was stirred at room temperature for several days. The completion of the reaction was monitored by NMR spectroscopy. After all volatile components were removed under reduced pressure, the product was obtained in nearly quantitative yield (>99%). For further purification, the crude product was sublimed. The desired product was obtained analytically pure as a colourless, crystalline solid.

1,2-Bis[(*E*)-2-(chlorodimethylsilyl)vinyl]benzene (2). Synthesis according to general procedure using precursor **1** (0.19 g, 1.5 mmol), chlorodimethylsilane (1.4 mL) and Et$_2$O (3 mL). Sublimation (80 °C, 10^{-3} mbar) of the crude product afforded colourless crystals of **2** in quantitative yield (0.47 g). ^{1}H NMR (500 MHz, C$_6$D$_6$): $\delta = 7.43$ (d, $^3J_{H,H} = 19$ Hz, 2H, C*H*=CH–Si), 7.28 (dd, $^3J_{H,H} = 6$ Hz, $^4J_{H,H} = 3$ Hz, 2H, H$_{ortho}$), 7.05 (dd, $^3J_{H,H} = 6$ Hz, $^4J_{H,H} = 3$ Hz, 2H, H$_{meta}$), 6.22 (d, $^3J_{H,H} = 19$ Hz, 2H, CH=C*H*–Si), 0.37 (s, 12H, C*H*$_3$) ppm; ^{13}C{^{1}H} NMR (126 MHz, C$_6$D$_6$): $\delta = 144.8$ (CH=CH–Si), 136.8 (C$_{ipso}$), 129.1 (CH=CH–Si), 128.8 (C$_{meta}$), 127.2 (C$_{ortho}$), 1.9 (CH$_3$) ppm; ^{29}Si{^{1}H} NMR (99 MHz, C$_6$D$_6$): $\delta = 18.3$ ppm; CHN analysis calcd (%) for C$_{14}$H$_{20}$Cl$_2$Si$_2$: C 53.32, H 6.39; found: C 53.20, H 6.48.

1,2-Bis[(*E*)-2-(dichloromethylsilyl)vinyl]benzene (3). Synthesis according to general procedure using precursor **1** (0.18 g, 1.4 mmol), dichloromethylsilane (1.2 mL) and Et$_2$O (3 mL). Sublimation (100 °C, 10^{-3} mbar) of the crude product afforded colourless crystals of **3** in

quantitative yield (0.50 g). ^{1}H NMR (500 MHz, C$_6$D$_6$): $\delta = 7.44$ (d, $^3J_{H,H} = 19$ Hz, 2H, C*H*=CH–Si), 7.09 (m, 2H, H$_{ortho}$), 6.99 (m, 2H, H$_{meta}$), 6.05 (d, $^3J_{H,H} = 19$ Hz, 2H, CH=C*H*–Si), 0.54 (s, 6H, C*H*$_3$) ppm; ^{13}C{^{1}H} NMR (126 MHz, C$_6$D$_6$): $\delta = 146.8$ (CH=CH–Si), 136.0 (C$_{ipso}$), 129.5 (C$_{meta}$), 127.4 (C$_{ortho}$), 126.1 (CH=CH–Si), 5.1 (CH$_3$) ppm; ^{29}Si{^{1}H} NMR (99 MHz, C$_6$D$_6$): $\delta = 17.1$ ppm; CHN analysis calcd (%) for C$_{12}$H$_{14}$Cl$_4$Si$_2$: C 40.46, H 3.96; found: C 40.41, H 4.07.

1,2-Bis[(*E*)-2-(trichlorosilyl)vinyl]benzene (4). Synthesis according to general procedure using precursor **1** (0.16 g, 1.3 mmol), trichlorosilane (3.0 mL) and Et$_2$O (9 mL). Sublimation (120 °C, 10^{-3} mbar) of the crude product afforded colourless crystals of **4** in quantitative yield (0.52 g). ^{1}H NMR (500 MHz, C$_6$D$_6$): $\delta = 7.49$ (d, $^3J_{H,H} = 19$ Hz, 2H, C*H*=CH–Si), 7.02 (m, 2H, H$_{ortho}$), 6.98 (m, 2H, H$_{meta}$), 5.97 (d, $^3J_{H,H} = 19$ Hz, 2H, CH=C*H*–Si) ppm; ^{13}C{^{1}H} NMR (126 MHz, C$_6$D$_6$): $\delta = 148.7$ (CH=CH–Si), 135.2 (C$_{ipso}$), 130.0 (C$_{meta}$), 127.6 (C$_{ortho}$), 123.7 (CH=CH–Si) ppm; ^{29}Si{^{1}H} NMR (99 MHz, C$_6$D$_6$): $\delta = -2.9$ ppm; CHN analysis calcd (%) for C$_{10}$H$_8$Cl$_6$Si$_2$: C 30.25, H 2.03; found: C 30.46, H 2.09.

1,2-Bis[(*E*)-2-(bis(perfluorophenyl)boraneyl)vinyl]benzene (5). 1,2-Diethynylbenzene (**1**, 11.2 mg, 88.8 μmol) was dissolved in benzene (1 mL) and Piers' borane (61.6 mg, 178 μmol) was added at room temperature. The resulting reaction mixture turned yellow and after a few minutes, the product crystallised from benzene. The crystalline solid was separated from the supernatant liquid and after removing all volatiles, 1,2-bis[(*E*)-2-(bis(perfluorophenyl)boranyl)vinyl]benzene (**5**) was isolated as a yellow crystalline solid in quantitative yield (72.6 mg). ^{1}H NMR (500 MHz, C$_6$D$_6$): $\delta = 7.73$ (d, $^3J_{H,H} = 18$ Hz, 2H, C*H*=CH–B), 7.39 (dd, $^3J_{H,H} = 6$ Hz, $^4J_{H,H} = 3$ Hz, 2H, H$_{ortho}$), 7.35 (d, $^3J_{H,H} = 18$ Hz, 2H, CH=C*H*–B), 7.01 (dd, $^3J_{H,H} = 6$ Hz, $^4J_{H,H} = 3$ Hz, 2H, H$_{meta}$) ppm; ^{13}C{^{1}H} NMR (126 MHz, C$_6$D$_6$): $\delta = 159.5$ (CH=CH–B), 147.9 (m, C^F), 143.7 (m, C^F), 137.8 (m, C^F), 137.5 (CH=CH–B), 131.3 (C$_{meta}$), 129.2 (C$_{ortho}$), 128.4 (C$_{ipso}$) ppm; ^{11}B NMR (160 MHz, C$_6$D$_6$): $\delta = 58.7$ ppm; ^{19}F NMR (470 MHz, C$_6$D$_6$): $\delta = -129.6$ (m, 2F, *o*-F), -146.9 (m, 1F, *p*-F), -161.0 (m, 2F, *m*-F) ppm; CHN analysis calcd (%) for C$_{34}$H$_8$B$_2$F$_{20}$·C$_6$H$_6$ C 53.61, H 1.58; found: C 51.70, H 1.36.

1,2-Bis[(*E*)-2-(bis(bis(trimethylsilyl)methyl)aluminyl)vinyl]benzene (6). 1,2-Diethynylbenzene (**1**, 68 mg, 0.54 mmol) was dissolved in *n*-hexane (7 mL) and bis[bis(trimethylsilyl)methyl]aluminium hydride (374 mg, 1.08 mmol) was added at room temperature. The resulting reaction mixture was stirred for 15 min. All volatile components were removed under reduced pressure, 1,2-bis[(*E*)-2-(bis(bis-(tri-methylsilyl)-methyl)aluminyl)vinyl]benzene (**6**) was obtained as a light-yellow solid in quantitative yield (0.44 g) after further drying in vacuum 6 h. ^{1}H NMR (500 MHz, C$_6$D$_6$): $\delta = 7.90$ (d, $^3J_{H,H} = 20$ Hz, 2H, C*H*=CH–Al), 7.70 (dd, $^3J_{H,H} = 6$ Hz, $^4J_{H,H} = 3$ Hz, 2H, H$_{ortho}$), 7.10 (dd, $^3J_{H,H} = 6$ Hz, $^4J_{H,H} = 3$ Hz, 2H, H$_{meta}$), 6.95 (d, $^3J_{H,H} = 20$ Hz, 2H, CH=C*H*–Al), 0.30 (s, 72H, C*H*$_3$), -0.19 (s, 4H, C*H*) ppm; ^{13}C{^{1}H} NMR (126 MHz, C$_6$D$_6$): $\delta = 147.9$ (CH=CH–Al), 141.5 (CH=CH–Al), 138.7 (C$_{ipso}$), 128.8 (C$_{meta}$), 126.6 (C$_{ortho}$), 10.6 (CH), 4.5 (CH$_3$) ppm; ^{29}Si{^{1}H} NMR (99 MHz, C$_6$D$_6$): $\delta = -3.6$ ppm; CHN analysis calcd (%) for C$_{38}$H$_{84}$Al$_2$Si$_8$: C 55.68, H 10.33; found: 54.26, H 10.78.

1,2 Bis[(diethylgallanyl)ethynyl]benzene (7). 1,2-Diethynylbenzene (**1**, 85 mg, 0.67 mmol) was dissolved in pure triethylgallium (0.3 mL) and stirred at room temperature for 7 d. At first, the reaction solution was a clear orange liquid; with increasing reaction time, the solution turned into an orange suspension. After removing the excess of triethylgallium under reduced pressure, 1,2-bis-[(diethylgallanyl)ethynyl]benzene (**7**) was isolated as an orange-brownish solid. Yield: 224 mg, 88%. ^{1}H NMR (500 MHz, THF-d$_8$): $\delta = 7.31$ (dd, $^3J_{H,H} = 6$ Hz, $^4J_{H,H} = 3$ Hz, 2H, H$_{ortho}$), 7.06 (dd, $^3J_{H,H} = 6$ Hz, $^4J_{H,H} = 3$ Hz, 2H, H$_{meta}$), 1.14 (t, $^3J_{H,H} = 8.1$ Hz, 12H, C*H*$_3$), 0.37 (q, $^3J_{H,H} = 8.1$ Hz, 8H, C*H*$_2$) ppm; ^{13}C{^{1}H} NMR (126 MHz, THF-d$_8$): $\delta = 133.3$ (C$_{ortho}$), 128.6 (C$_{ipso}$), 127.1 (C$_{meta}$), 109.7 (*C*≡CB), 107.2 (C≡*C*B), 10.9 (CH$_3$), 4.7

ChemistryOpen

Full Papers
doi.org/10.1002/open.202100198

Chemistry Europe
European Chemical
Societies Publishing

(CH$_2$) ppm; CHN analysis calcd (%) for C$_{18}$H$_{24}$Ga$_2$: C 56.92, H 6.37; found: C 57.29, H 6.70.

Crystal Structure Determination. Suitable crystals of **2**, **3** and **4** were obtained by sublimation. Suitable crystals of compound **5** were obtained from benzene at room temperature. Compound **6** could be crystallised from a saturated benzene solution with two equivalents of pyridine by continuous concentration. Suitable crystals of compound **7** were obtained from benzene. The condensation product **7 a** was obtained crystalline by a dissolution experiment in CD$_2$Cl$_2$/C$_6$D$_6$, with pyridine added to the suspension through slow diffusion. The crystals were selected inside a glovebox, coated with Paratone N oil, mounted on a glass fibre and transferred onto the goniometer of the diffractometer into a nitrogen gas cold stream to solidify the oil. Data collection was performed with an Agilent Supernova diffractometer. Using Olex2[30], the structures were solved with ShelXT[31] using intrinsic phasing and refined with the ShelXL[32] refinement package using least squares minimisation. The crystal and refinement details are listed in Table 3.

Acknowledgements

Conflict of Interest

The authors declare no conflict of interest.

[1] C. J. Pedersen, *Angew. Chem. Int. Ed. Engl.* **1988**, *27*, 1021–1027.
[2] J.-M. Lehn, *Angew. Chem. Int. Ed. Engl.* **1988**, *27*, 89–112.
[3] D. J. Cram, *Angew. Chem. Int. Ed. Engl.* **1988**, *27*, 1009–1112.
[4] a) J. R. Hyde, T. J. Karol, J. P. Hutchinson, H. G. Kuivila, J. Zubieta, *Organometallics* **1982**, *1*, 404–405; b) M. Austin, K. Gebreyes, H. G. Kuivila, K. Swami, J. A. Zubieta, *Organometallics* **1987**, *6*, 834–842.
[5] a) L. Hong, S. Ahles, A. H. Heindl, G. Tiétcha, A. Petrov, Z. Lu, C. Logemann, H. A. Wegner, *Beilstein J. Org. Chem.* **2018**, *14*, 618–625; b) L. Schweighauser, H. A. Wegner, *Chem. Eur. J.* **2016**, *22*, 14094–14103; c) E. von Grotthuss, S. E. Prey, M. Bolte, H.-W. Lerner, M. Wagner, *Angew. Chem. Int. Ed.* **2018**, *57*, 16491–16495; *Angew. Chem.* **2018**, *130*, 16729–16733; d) Z. Lu, L. Schweighauser, H. Hausmann, H. A. Wegner, *Angew. Chem. Int. Ed.* **2015**, *54*, 15556–15559; *Angew. Chem.* **2015**, *127*, 15777–15780; e) S. E. Prey, M. Wagner, *Adv. Synth. Catal.* **2021**, *363*, 2290–2309.
[6] a) F. Jäkle, *Chem. Rev.* **2010**, *110*, 3985–4022; b) C. Hoffend, F. Schödel, M. Bolte, H.-W. Lerner, M. Wagner, *Chem. Eur. J.* **2012**, *18*, 15394–15405.
[7] A. K. Holliday, A. G. Massey, *J. Chem. Soc.* **1960**, 43–46.
[8] a) W. Uhl, F. Hannemann, W. Saak, R. Wartchow, *Eur. J. Inorg. Chem.* **1998**, 921–926; b) W. Uhl, F. Hannemann, *J. Organomet. Chem.* **1999**, *579*, 18–23.
[9] a) K. Swami, J. P. Hutchinson, H. G. Kuivila, J. A. Zubieta, *Organometallics* **1984**, *3*, 1687–1694; b) M. M. Naseer, K. Jurkschat, *Chem. Commun.* **2017**, *53*, 8122–8135.
[10] A. S. Wendji, C. Dietz, S. Kühn, M. Lutter, D. Schollenmeyer, W. Hiller, K. Jurkschat, *Chem. Eur. J.* **2016**, *22*, 404–416.
[11] a) J. D. Beckwith, M. Tschinkl, A. Picot, M. Tsunoda, R. Bachmann, F. P. Gabbaï, *Organometallics* **2001**, *20*, 3169–3174; b) H. Schmidbaur, H.-J. Öller, D. L. Wilkinson, B. Huber, G. Müller, *Chem. Ber.* **1989**, *122*, 31–36.
[12] R. Altmann, K. Jurkschat, M. Schürmann, D. Dakternieks, A. Duthie, *Organometallics* **1998**, *17*, 5858–5866.
[13] K. Tamao, T. Hayashi, Y. Ito, M. Shiro, *Organometallics* **1992**, *11*, 2099–2114.
[14] H. E. Katz, *J. Org. Chem.* **1989**, *54*, 2179–2183.
[15] E. A. Jeffery, T. Mole, *J. Organomet. Chem.* **1968**, *11*, 393–398.
[16] a) J. Chmiel, B. Neumann, H.-G. Stammler, N. W. Mitzel, *Chem. Eur. J.* **2010**, *16*, 11906–11914; b) J. Horstmann, M. Hyseni, A. Mix, B. Neumann, H.-G. Stammler, N. W. Mitzel, *Angew. Chem. Int. Ed.* **2017**, *56*, 6107–6111; *Angew. Chem.* **2017**, *129*, 6203–6207.
[17] a) W. Uhl, M. Matar, *J. Organomet. Chem.* **2002**, *664*, 110–115; b) W. Uhl, J. Bohnemann, D. Heller, A. Hepp, M. Lyah, *Z. Anorg. Allg. Chem.* **2012**, *638*, 68–75.
[18] a) W. Uhl, M. Claesener, S. Haddadpour, B. Jasper, A. Hepp, *Dalton Trans.* **2007**, 417–423; b) W. Uhl, A. Hepp, H. Westenberg, S. Zemke, E.-U. Würthwein, J. Hellmann, *Organometallics* **2010**, *29*, 1406–1412.
[19] J.-H. Lamm, J. Horstmann, J. H. Nissen, J.-H. Weddeling, B. Neumann, H.-G. Stammler, N. W. Mitzel, *Eur. J. Inorg. Chem.* **2014**, 4294–4301.
[20] A. Schwartzen, L. Siebe, J. Schwabedissen, B. Neumann, H.-G. Stammler, N. W. Mitzel, *Eur. J. Inorg. Chem.* **2018**, 2533–2540.
[21] See for example: S. Jana, F. He, R. M. Koenigs, *Org. Lett.* **2020**, *22*, 4873–4877.
[22] J. Horstmann, M. Niemann, K. Berthold, A. Mix, B. Neumann, H.-G. Stammler, N. W. Mitzel, *Dalton Trans.* **2017**, *46*, 1898–1913.
[23] a) S. W. Carr, M. Motevalli, D. L. Ou, A. C. Sullivan, *J. Mater. Chem.* **1997**, *7*, 865–872; b) N. W. Mitzel, P. T. Brain, M. A. Hofmann, D. W. H. Rankin, R. Schröck, H. Schmidbaur, *Z. Naturforsch.* **2002**, *57b*, 202–214; c) J. E. Laska, P. Kaszynski, *Organometallics* **1998**, *17*, 2018–2026.
[24] a) D. J. Parks, R. E. v. H. Spence, W. E. Piers, *Angew. Chem. Int. Ed. Engl.* **1995**, *34*, 809–811; b) D. J. Parks, W. E. Piers, G. P. A. Yap, *Organometallics* **1998**, *17*, 5492–5503.
[25] W. Uhl, H. R. Bock, M. Claesener, M. Layh, I. Tiesmeyer, E.-U. Würthwein, *Chem. Eur. J.* **2008**, *14*, 11557–11564.
[26] W. Uhl, E. Er, A. Hepp, J. Kösters, J. Grunenberg, *Organometallics* **2008**, *27*, 3346–3351.
[27] W. Uhl, F. Breher, S. Haddadpour, R. Koch, M. Matar, *Z. Anorg. Allg. Chem.* **2004**, *630*, 1839–1845.
[28] K. P. C. Vollhardt, N. E. Schore, *Organische Chemie*, 4. Aufl., Wiley-VCH, Weinheim, **2005**.
[29] W. Uhl, L. Cuypers, R. Graupner, J. Molter, A. Vester, B. Neumüller, *Z. Anorg. Allg. Chem.* **2001**, *627*, 607–614.
[30] O. V. Dolomanov, L. J. Bourhis, R. J. Gildea, J. A. K. Howard, H. Puschmann, *J. Appl. Crystallogr.* **2009**, *42*, 339–341.
[31] G. M. Sheldrick, *Acta Crystallogr.* **2015**, *A71*, 3–8.
[32] G. M. Sheldrick, *Acta Crystallogr.* **2015**, *C71*, 3–8.